Mechanism of the T286A-Mutant αCaMKII Interactions with Ca^{2+}/Calmodulin and ATP†

Athanasios Tzortzopoulos and Katalin Török*

Department of Basic Medical Sciences, St George's Hospital Medical School, London SW17 0RE, U.K.

Received December 11, 2003; Revised Manuscript Received March 12, 2004

ABSTRACT: The role of adenosine 5′-triphosphate (ATP) in the activation mechanism of α-Ca^{2+}/calmodulin-dependent protein kinase II (αCaMKII) was investigated using the T286A non-autophosphorylatable mutant of αCaMKII. Characterization of the T286A-αCaMKII mutant revealed $k_{cat} = 0.06 \pm 0.02$ s^{-1} for the T286A mutant, a 6 (± 2)-fold lower value compared to wild-type αCaMKII with 100 μM smooth muscle myosin light chain (MLC) as substrate. MLC phosphorylation by the T286A mutant and wild-type αCaMKII was cooperative, with Hill coefficients 2.3 ± 0.1 and 2.4 ± 0.3, respectively. K_m values for MLC were 96 ± 28 μM with T286A-αCaMKII and 49 ± 29 μM for wild-type αCaMKII. Thus, while the activity of αCaMKII was sensitive to mutation of the Thr_{286} residue to Ala, the mechanisms of the wild-type and T286A mutant enzyme appeared similar. K_d for Ca^{2+}/calmodulin was 2-fold reduced to 40 nM compared to that of wild-type αCaMKII (75 nM). ATP induced a 9-fold stabilization of Ca^{2+}/calmodulin binding to the T286A mutant enzyme. Fluorescence stopped-flow kinetic experiments revealed that two Ca^{2+}/calmodulin−enzyme complexes were formed, the first, unaffected by ATP, with association and dissociation rate constants of 2×10^7 M^{-1} s^{-1} and 5 s^{-1}, respectively, containing calmodulin in extended conformation. The second complex, in which calmodulin adopted a compact conformation, was formed with association rate constant 3×10^6 M^{-1} s^{-1} and dissociation at 0.15 s^{-1} in the absence and 0.015 s^{-1} in the presence of ATP. These data show that ATP is involved in the activation mechanism by forming two classes of Ca^{2+}/calmodulin·αCaMKII·ATP complex. It is likely that only one of the complexes is on the activation pathway.

Ca^{2+}/calmodulin-dependent protein kinase II isoform α (αCaMKII)[1] is a major protein transducer of the upstream Ca^{2+} and calmodulin signals in neurons (*1*, *2*). αCaMKII is a homo-oligomeric enzyme consisting of 12 identical α subunits arranged as two stacked concentric hexameric rings formed by the C-terminal association domains of each monomer (*3*, *4*). The higher-order oligomeric organization of this protein kinase is tightly coupled to its unique functional and regulatory properties. αCaMKII function is necessary and sufficient for the induction of LTP (*1*), a model for long-lasting increases in synaptic strength likely to play important roles in learning and memory (*5*). αCaMKII is able to translocate to (*6*) and co-localize with the NR2B subunit of *N*-methyl-D-aspartate (NMDA) receptor to the postsynaptic density, where it is thought to respond to local Ca^{2+} signals (*7*) and mediate LTP and synaptic plasticity by modulating NMDA receptor inactivation (*8*) and α-amino-3-hydroxy-5-methyl-4-isoxazolepropionic acid (AMPA) receptor-mediated rapid excitatory synaptic transmission (*9*, *10*). The role of αCaMKII in spatial learning and memory has been demonstrated by experiments using transgenic mice deficient in αCaMKII (*11*, *12*). Furthermore, the role of site-specific Thr_{286}-autophosphorylation of αCaMKII in spatial learning has been shown in behavioral studies of transgenic mice expressing the non-autophosphorylatable (T286A) mutant analogue of αCaMKII (*13*, *14*).

Autophosphorylation is a unique feature of αCaMKII, which is critical for the regulation of the enzyme (*15*). Thr_{286} is the major regulatory autophosphorylation site in αCaMKII that resides in the autoinhibitory domain. A number of studies suggest that αCaMKII forms a weak complex with calmodulin and that Ca^{2+}/calmodulin-dependent Thr_{286}-autophosphorylation leads to calmodulin "trapping" (*16*, *17*). Thr_{286}-autophosphorylation of wild-type αCaMKII is thought to generate an enzyme which is active even in the absence of bound Ca^{2+}/calmodulin (*18*). It has been previously shown

† This work is supported by Wellcome Trust Grant 048458 and MRC Grant G9803105 to K.T.

* Address correspondence to Dr. K. Török, Department of Basic Medical Sciences, St George's Hospital Medical School, Cranmer Terrace, London SW17 0RE, UK. Phone +44 208 725 5832. Fax: +44 208 725 3581. E-mail: k.torok@sghms.ac.uk.

[1] Abbreviations: ADP, adenosine 5′-diphosphate; IAEDANS, 5-(2-iodoacetyl)amino-ethylamino-naphthalene-1-sulfonic acid; AMP-PNP, 5′-adenylyimidodiphosphate; ATP, adenosine 5′-triphosphate; αCaMKII, α-Ca^{2+}/calmodulin-dependent protein kinase II; αCaMKII-Thr_{286}-P, Thr_{286}-phospho-αCaMKII; DA-calmodulin, DDP-maleimide- and AEDANS-substituted-T34C,T110C-calmodulin; DDP-maleimide, *N*-(4-dimethylamino-3,5-dinitrophenyl)-maleimide; DTT, 1,4-dithiothreitol; EDTA, ethylenediamine-*N*,*N*,*N*′,*N*′-tetraacetic acid; EGTA, 1,2-bis(2-aminoethoxy)ethane *N*,*N*,*N*′,*N*′-tetraacetic acid; HPLC, high-pressure liquid chromatography; LDH, lactate dehydrogenase; MLC, chicken gizzard smooth muscle myosin light chain; NADH, reduced nicotinamide adenine dinucleotide; PBS, phosphate-buffered saline pH 7.4; PEP, phosphoenolpyruvate; PIPES, piperazine-*N*,*N*′-bis(2-ethanesulfonic acid); PK, pyruvate kinase; PMSF, phenylmethylsulfonyl fluoride; TA-calmodulin or TA-cal, 2-chloro-(ϵ-amino-Lys75)-[6-(4-*N*,*N*-diethylaminophenyl)-1,3,5-triazin-4-yl]-calmodulin; TA-Cl, 2,4-dichloro-6-(4-*N*,*N*-diethylaminophenyl)-1,3,5-triazine; Tris, tris(hydroxymethyl)-aminomethane.

10.1021/bi036224m CCC: $27.50
Published on Web 05/05/2004

that calmodulin trapping does not occur in the T286A point mutant (*16*). It has also been shown that the T286A point mutant does not exhibit any Ca^{2+}/calmodulin-independent activity (*19*) unless it is bound to the NR2B subunit of the NMDA receptor (*20*).

The kinetic mechanism of brain CaMKII has been studied by steady-state enzyme kinetic methods. Rapid equilibrium random (*21*) and ordered (*22*) mechanisms have been described with protein and peptide substrates, respectively. There is controversy regarding ATP binding to αCaMKII in the inactive state, in the absence of Ca^{2+}/calmodulin. While steady-state analysis has suggested that ATP cannot bind to inactive αCaMKII (*23*), transient kinetic studies are consistent with the existence of an αCaMKII.ATP complex (*17*).

We have previously shown that ATP affects the interactions of Ca^{2+}/calmodulin with αCaMKII and suggested that both ATP binding and the resulting Thr_{286}-autophosphorylation contribute to these effects (*17*). To investigate the effects of ATP binding on the conformation as well as the affinity of Ca^{2+}/calmodulin to αCaMKII independently of Thr_{286}-autophosphorylation, we used the T286A mutant of αCaMKII. The steady-state activation properties of T286A-αCaMKII were characterized and compared with those of wild-type αCaMKII. The interactions of fluorescently labeled calmodulin derivatives with the mutant enzyme were studied in comparison with the wild-type enzyme using stopped-flow spectroscopies.

MATERIALS AND METHODS

Proteins and Peptides. Recombinant baculovirus for the overexpression of T286A mutant was a kind gift from Dr. D. A. Brickey and Professor T. R. Soderling (Vollum Institute, Oregon Health and Science University, Portland, OR). T286A-αCaMKII mutant was expressed and purified as described for wild-type αCaMKII (*17*). The yield typically was 2 mg of T286A-αCaMKII mutant from a 200-mL suspension culture of Sf9 cells. The protein was rapidly frozen in liquid nitrogen and stored at −80 °C. TA-cal and DA-cal were prepared as previously described (*17*, *24*). Pig brain calmodulin was purified as previously described (*24*) and was used in stopped-flow experiments to displace TA-cal and DA-cal. A previously developed high-yield MLC overexpression system in BL-21 cells was utilized, and purification was carried out as described in ref *25*. αCaMKII peptide, residues 281−319, was synthesized by P. Fletcher (National Institute for Medical Research, London, UK) and purified by reversed-phase HPLC to homogeneity. Its identity was checked and confirmed by mass spectrometry.

The concentration of T286A-αCaMKII was measured using $\epsilon_o = 64\,805\ M^{-1}\ cm^{-1}$ (280 nm), calculated from the amino acid composition (*26*). The Bradford assay was also used with bovine serum albumin as standard (*27*). The results of the two protein assays were identical within 10%. $\epsilon_o = 1800\ M^{-1}\ cm^{-1}$ (278 nm) in 2 mM EGTA was used for pig brain calmodulin and T34C/T110C-calmodulin, and $\epsilon_o = 4400\ M^{-1}\ cm^{-1}$ (278 nm) was used for MLC calculated from the amino acid composition (*26*). αCaMKII peptide, residues 281−319, was measured by weight.

Spectroscopy. Experiments were carried out at 21 °C unless otherwise specified. The assay solution contained 50 mM K-PIPES pH 7.0, 100 mM KCl, 2 mM $MgCl_2$, 1 mM DTT, and 500 μM $CaCl_2$, unless otherwise stated. DA-cal ($\lambda_{ex} = 335$ nm and $\lambda_{em} = 500$ nm) and TA-cal ($\lambda_{ex} = 365$ nm and $\lambda_{em} = 415$ nm) emission spectra were recorded on an SLM spectrofluorimeter.

Fluorescence stopped-flow measurements were carried out using a Hi-Tech PQ/SF-53 double-mixing apparatus (Hi-Tech Scientific, UK) set to $\lambda_{ex} = 363$ nm and $\lambda_{em} > 455$ nm for experiments with DA-cal and $\lambda_{em} > 400$ nm for TA-cal. Concentrations are given in the mixing chamber. A Perkin-Elmer spectrophotometer and an SLM spectrofluorimeter were used for absorption and other fluorescence measurements. In all experiments, fluorescence was normalized so that Ca^{2+}/DA-cal or Ca^{2+}/TA-cal fluorescence corresponded to 1 and buffer fluorescence to 0.

Software. The steady-state kinetic data were analyzed using GRAFIT v. 4.0 and fitted to the Michaelis−Menten equation, $V = V_{max}[S]/(K_m + [S])$, or the Hill equation, $V = V_{max}[S]^n/(K_m + [S]^n)$. The Hi-Tech RK-2 program was used to acquire and analyze the stopped-flow kinetic data. KSIM (by Neil Millar) was used to generate simulated kinetic reactions.

Enzyme Activity. Steady-state protein kinase activities of wild-type and T286A mutant αCaMKII, stimulated by calmodulin and DA-calmodulin, were measured using MLC as target. A continuous enzyme-linked fluorescence assay was used to determine ADP production, linked to NADH oxidation with a 1:1 stoichiometry (*28*). The reactions were carried out at 21 °C. The 0.5-mL assay solution contained 50 mM K-PIPES pH 7.0, 100 mM KCl, 5 mM DTT, 2 mM $MgCl_2$, 2 mM PEP, 500 μM $CaCl_2$, 4.5 units of LDH (bovine heart), 2 units of PK (rabbit muscle), and 10.8 μM NADH. The concentrations of ATP calmodulin and MLC were varied as specified. λ_{ex} was 340 nm, and λ_{em} was set to 460 nm (for NADH). When DA-cal was added in the reaction mixture, λ_{em} was set to 420 nm where DA-cal emission was negligible, thus avoiding interference with NADH fluorescence emission.

DA-cal and pig brain calmodulin were compared in steady-state assays of phosphorylation of MLC target by T286A-αCaMKII mutant. At 37.5 nM enzyme concentration, 1 mM ATP, 100 μM MLC, and pig brain calmodulin or DA-cal at ≥0.5 μM, the activities were 56 ± 6 nmol of ADP min^{-1} (mg of enzyme)$^{-1}$ stimulated by calmodulin and 61 ± 8 nmol of ADP min^{-1} (mg of enzyme)$^{-1}$ stimulated by DA-cal.

MLC binding to calmodulin was not detected by TA-cal fluorescence; however, as high MLC concentrations were used in the enzyme assay, we tested MLC binding to calmodulin by additional methods. Calmodulin−Sepharose chromatography revealed that some MLC bound in a Ca^{2+}-dependent manner. Fluorescence polarization measurements were then carried out to quantify the binding affinity. Fluorescein-labeled calmodulin labeled on residue Lys_{75} (FL-cal) (*29*), the same site as in TA-cal, was used because its fluorescence responds by increased polarization to αCaMKII binding (K. Török, unpublished data). MLC up to 305 μM was tested for Ca^{2+}/FL-cal binding. A K_d value of 75 μM was derived from the anisotropy change of 0.04. It was then investigated how this binding affected our enzyme kinetic measurements. These experiments were all carried out at 5 μM $[cal]_o$. It was calculated that MLC binding removed up to 3.7 μM calmodulin at 220 μM MLC from the solution.

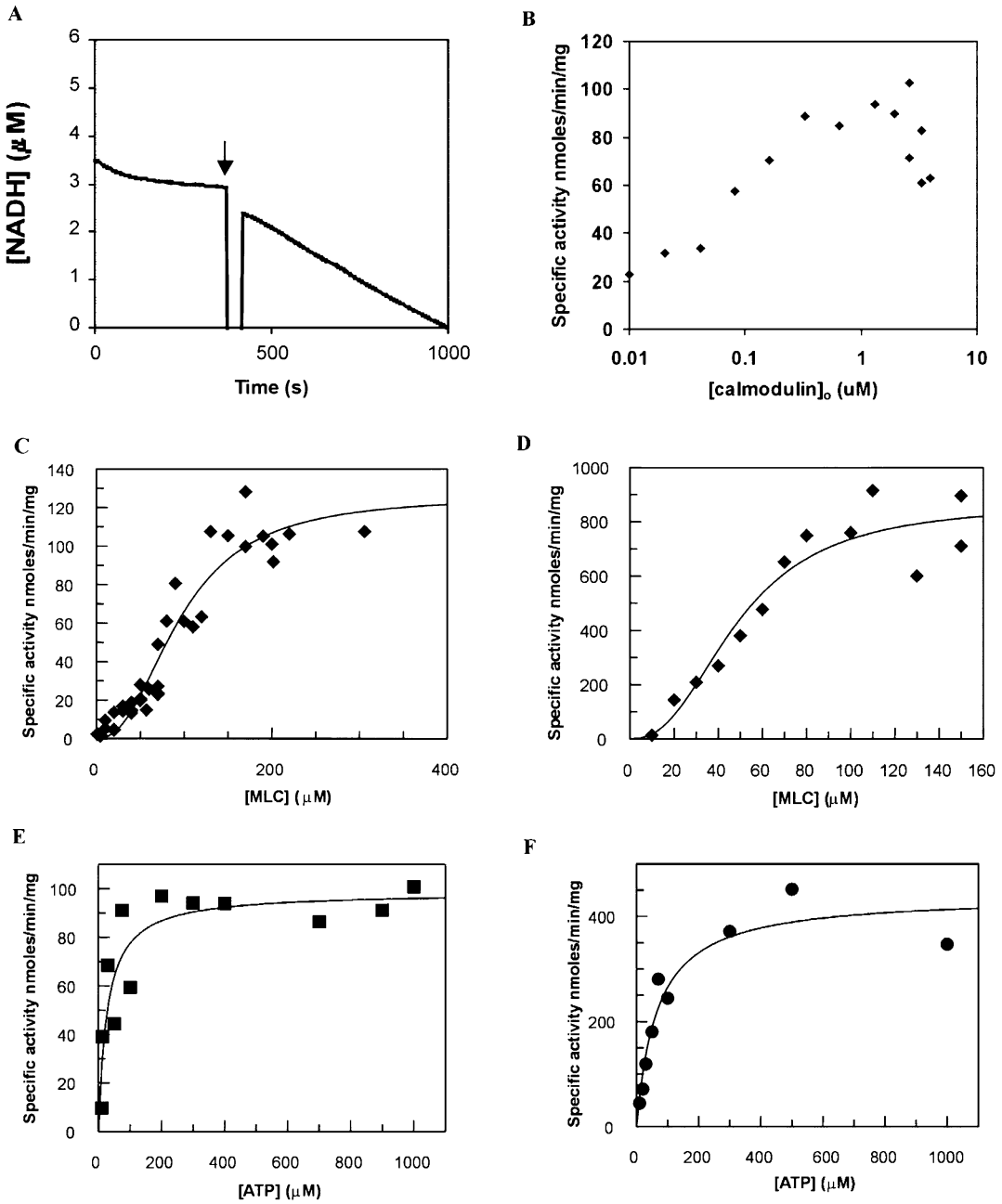

FIGURE 1: NADH-coupled substrate concentration dependence of steady-state activities of T286A-αCaMKII and wild-type enzyme. All steady-state parameters are listed in Table 1. (A) Measurement of the specific activity of the T286A mutant enzyme: 0.2 μM T286A mutant, 500 μM Ca^{2+}, 5 μM calmodulin, 40 μM MLC, and 1 mM ATP were present in the assay mix at 21 °C. Enzyme was added last to start the reaction. The specific activity of the T286A mutant enzyme was 19 nmol min^{-1} mg^{-1}. (B) Calmodulin concentration dependence of T286A-αCaMKII steady-state activity: 0.2 μM T286A mutant, 100 μM MLC, and 1 mM ATP were present in the assay mix. (C,D) MLC concentration dependence of the steady-state activities of T286A-αCaMKII and wild-type αCaMKII, respectively: 0.1 or 0.2 μM enzyme, 1 mM ATP, and 5 μM Ca^{2+}/calmodulin were present in the assay mix. (E,F) ATP concentration dependence of the steady-state activities of T286A-αCaMKII and wild-type αCaMKII, respectively: 0.1 or 0.2 μM enzyme, 100 μM MLC, and 5 μM Ca^{2+}/calmodulin were present in the assay mix.

At the typically used 100 μM MLC concentration, 2.8 μM calmodulin was bound to MLC. Thus, even at the highest MLC concentrations used, the calmodulin concentrations available for enzyme activation were >1.3 μM and typically 2.2 μM. The calmodulin concentrations were thus not critically reduced by MLC binding in our assays and represented saturating concentrations for the wild-type and mutant enzymes. Calmodulin concentrations were corrected for MLC binding in Figure 1B, and the corrected plot is shown. MLC concentrations for the assays in Figure 1C,D were also corrected for calmodulin binding and reanalyzed. The analysis showed that this correction did not noticeably affect the fitted values.

RESULTS

Comparison of the Steady-State Kinetics of Wild-Type and T286A Mutant αCaMKII. The T286A mutant of αCaMKII was expressed in baculovirus-transfected insect cells and purified to homogeneity by the method previously developed for wild-type αCaMKII enzyme (*17*). Electron micrographic images of negatively stained T286A-αCaMKII mutant protein had a similar appearance to those of dodecameric

Table 1: Kinetic Constants of MLC Phosphorylation by T286A Mutant and Wild-Type αCaMKII Enzymes

	T286A			αCaMKII		
	$S_{0.5}$ (μM)	n^a	$V_{max}{}^b$	$S_{0.5}$ (μM)	n^a	$V_{max}{}^b$
Cal	<0.100		84 ± 6			
ATP	27 ± 9		99 ± 7	66 ± 18		440 ± 37
MLC	96 ± 28	2.3 ± 0.1	126 ± 8	49 ± 29	2.4 ± 0.3	866 ± 76

[a] *n* denotes Hill coefficient. The values for *n* represent the best-fit values to the Hill equation $v = V_{max}[S]^n/(K_m + [S]^n)$. Fixing *n* at 2 did not significantly alter the best-fit V_{max} and $S_{0.5}$ values. [b] V_{max} represents the enzyme specific activity at 100 μM MLC expressed in nanomoles per minute per milligram of enzyme.

αCaMKII (data not shown). Steady-state kinase activities of both the T286A-αCaMKII mutant and wild-type αCaMKII enzyme were determined in an NADH-coupled assay, measuring ADP release with MLC as substrate (*28*). We have previously determined that Thr_{286}-autophosphorylation of wild-type αCaMKII enzyme does not occur in the presence of >30 μM MLC (Tzortzopoulos et al., *Biochemistry*, in press). A steady-state assay of T286A mutant activity is shown in Figure 1A. Typically, the reaction was started by the addition of enzyme. In the absence of calmodulin, the enzyme activity was <2% of that measured in its presence for both the T286A mutant and wild-type αCaMKII (*17*). Steady-state kinetic parameters of both the T286A-αCaMKII mutant and wild-type enzymes were determined. Figure 1B−F shows the steady-state activities of the T286A-αCaMKII mutant and wild-type enzyme as a function of calmodulin, MLC, and ATP concentrations.

The steady-state kinase activity of the T286A mutant was measured at various calmodulin concentrations (range 0−5 μM) using 0.5 mM Ca^{2+}, 1 mM ATP, and 100 μM MLC. The best-fit V_{max} value for the T286A mutant enzyme was 84 ± 6 nmol min^{-1} mg^{-1}. Determination of the K_m for calmodulin was not possible at the enzyme concentration of 200 nM. An $S_{0.5}$ value of <100 nM was thus estimated (Figure 1B, Table 1).

Steady-state rates of T286A mutant and wild-type αCaMKII activities were determined over a range of MLC concentrations. At 5 μM calmodulin and 1 mM ATP, V_{max} values for MLC were 126 ± 8 nmol min^{-1} mg^{-1} T286A mutant and 866 ± 76 nmol min^{-1} mg^{-1} wild-type αCaMKII, revealing a ratio 6 ± 2 in the k_{cat} values for the wild-type and mutant enzymes Steady-state activation of both enzymes showed positive cooperativity as a function of MLC concentration and was best fit with K_m values for MLC of 96 ± 28 μM with the T286A mutant and 49 ± 29 μM with wild-type αCaMKII. For MLC, Hill coefficients of 2.3 ± 0.2 for the mutant and 2.4 ± 0.3 for the wild-type αCaMKII were obtained (Figure 1C,D, Table 1).

The ATP concentration dependence of the T286A mutant and αCaMKII steady-state activities in the presence of 5 μM calmodulin and 100 μM MLC gave V_{max} values of 99 ± 7 nmol min^{-1} mg^{-1} for the T286A mutant and 440 ± 37 nmol min^{-1} mg^{-1} for wild-type αCaMKII. The K_m values for ATP were 27 ± 9 μM for the T286A mutant and 66 ± 18 μM for wild-type αCaMKII (Figure 1E,F, Table 1). Thus, detailed examination revealed differences in both turnover rate and substrate affinities between the T286A mutant and wild-type αCaMKII enzymes.

Ca^{2+}/TA-cal Interactions with T286A-aCaMKII Mutant and Its ATP Complex by Stopped-Flow Kinetics. The effect of ATP on the kinetics of association and dissociation of Ca^{2+}/calmodulin from the non-autophosphorylatable T286A mutant was studied by fluorescence stopped-flow. A Lys_{75}-derivatized fluorescent calmodulin, TA-cal (*24*), was used to study its interactions with T286A-αCaMKII in the presence of Ca^{2+}. In association experiments, the fluorescence of Ca^{2+}/TA-cal changed in a biphasic process by T286A-αCaMKII binding (Figure 2A,B). Ca^{2+}/TA-cal fluorescence initially increased rapidly from relative fluorescence 1 (which is the normalized Ca^{2+}/TA-cal fluorescence) to 1.30, and then fell in a slower process to the value of 1.02. In the presence of ATP, similar fluorescence changes occurred, although the relative fluorescence values were somewhat different. The initial rise reached a maximum at 1.18, and the final fluorescence was 0.71 (Figure 2A,B). Both in the absence and in the presence of ATP, the rate of the initial rising phase was concentration dependent (Figure 2C,D). The gradient of k_{obs1} of the rapid rising phase as a function of T286A mutant concentration was 2.0 (± 0.2) × 10^7 M^{-1} s^{-1} in the absence and 1.9 (± 0.2) × 10^7 M^{-1} s^{-1} in the presence of ATP. The intercepts of the extrapolated linear plots of k_{obs1} versus [T286A mutant] are 7.8 ± 1.9 (Figure 2C) and 7.9 ± 1.2 s^{-1} in the presence of ATP (Figure 2D). The rate of the second, slow phase appeared to be concentration independent at 0.78 ± 0.05 s^{-1} in the absence of ATP. In the presence of ATP (Figure 2C), however, a better fit was obtained with two exponentials: the first rate was concentration dependent, with a gradient of (2.3 ± 0.1) × 10^6 M^{-1} s^{-1}, while the second process was concentration independent, at 0.45 ± 0.05 s^{-1} (Figure 2D).

Dissociation of Ca^{2+}/TA-cal.T286A-αCaMKII was measured by monitoring Ca^{2+}/TA-cal fluorescence changes upon its displacement from the T286A-αCaMKII and the ATP-bound T286A-αCaMKII complexes by pig brain calmodulin (Figure 2E,F). Ca^{2+}/TA-cal fluorescence changed in a biphasic manner upon dissociation from the nucleotide-free αCaMKII complex. The fluorescence first decreased to 0.95 at a rate k_{diss1} = 6.0 ± 0.9 s^{-1}, and subsequently increased to 1 at a rate k_{diss2} = 0.15 s^{-1} (Figure 2E). In contrast to the nucleotide-free Ca^{2+}/TA-cal.T286A-αCaMKII complex, dissociation of Ca^{2+}/TA-cal from ATP-bound Ca^{2+}/TA-cal.T286A complex was described by a monophasic Ca^{2+}/TA-cal fluorescence increase with k_{diss} = 0.015 ± 0.001 s^{-1} from relative fluorescence 0.71 to 1, which corresponds to normalized free Ca^{2+}/TA-cal fluorescence (Figure 2F). The biphasic dissociation curve in Figure 2E indicates a well-poised equilibrium between the two Ca^{2+}/cal.T286A-αCaMKII complexes, as the decay of both complexes can be observed. The monophasic dissociation curve in Figure 2F indicates that the equilibrium is strongly biased toward one of the complexes.

Mechanism of Ca^{2+}/TA-cal Interactions with T286A-αCaMKII Mutant and Its ATP Complex. The association kinetics presented in Figure 2C show a mechanism of interaction of TA-cal with the T286A mutant enzyme in which rapid binding is followed by slow isomerization. Relative fluorescence initially increases and then decreases but remains >1 throughout association. The fluorescence in the dissociation process of the Ca^{2+}/TA-cal.T286A complex, however, drops below the value of 1. Thus, one of the

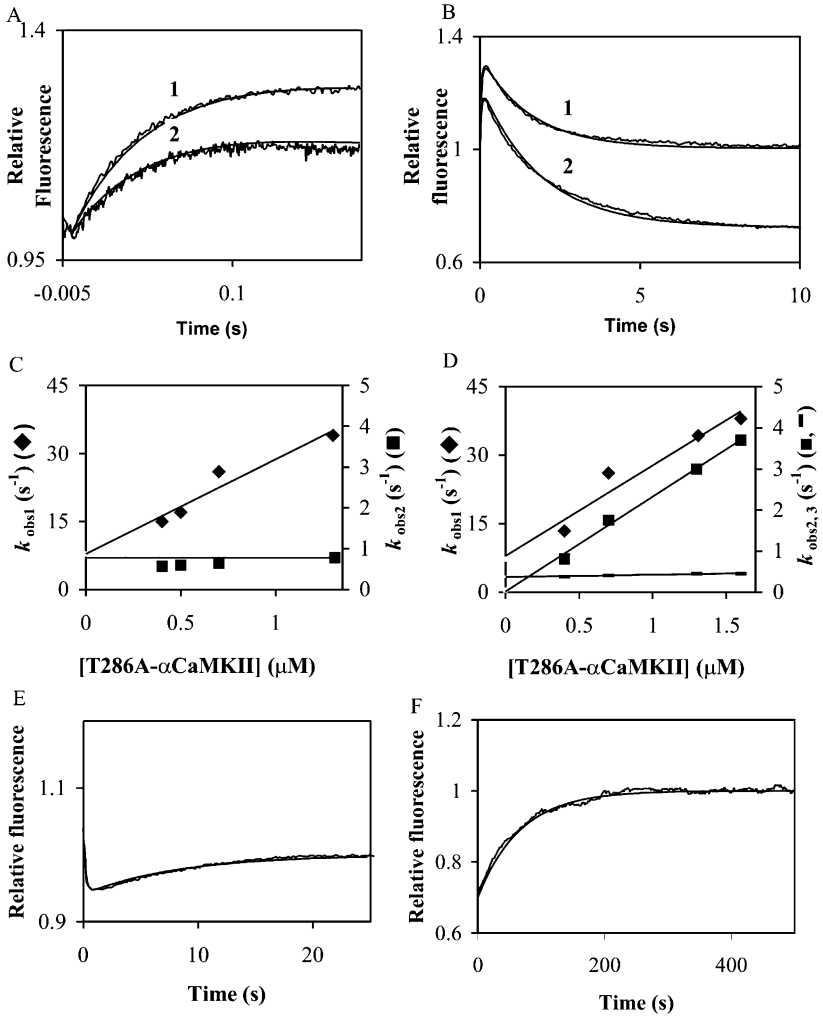

FIGURE 2: Association and dissociation kinetics of Ca^{2+}/TA-cal and T286A-αCaMKII. Fluorescence was monitored at $\lambda_{ex} = 365$ nm and $\lambda_{em} > 400$ nm, and the conditions were as described in Materials and Methods. (A,B) Association of Ca^{2+}/TA-cal and T286A-αCaMKII in the presence (records 2) and absence (records 1) of ATP on a short (A) and a long (B) time scale. The solid line shows the exponential fit to the experimental data. For record 1, 25 nM Ca^{2+}/TA-cal was rapidly mixed with 0.7 μM T286A-αCaMKII (concentrations in mixing chamber) in a stopped-flow fluorimeter. The rate constants of the two exponentials shown were $k_{obs1} = 26.0 \pm 0.5$ s^{-1} (rising fluorescence) and $k_{obs2} = 0.60 \pm 0.01$ s^{-1} (decreasing fluorescence). The fluorescence started from 1 (F_1) and rose to 1.30 (F_2), and equilibrium was achieved at 1.02 (F_∞). For record 2, 25 nM Ca^{2+}/TA-cal was rapidly mixed with 0.7 μM T286A-αCaMKII and 0.5 mM ATP. The rate constants of the two exponentials shown were $k_{obs1} = 32.0 \pm 1.1$ s^{-1} (rising fluorescence) and $k_{obs2} = 0.50 \pm 0.01$ s^{-1} (decreasing fluorescence). The fluorescence started from 1 (F_1) and rose to 1.18 (F_2), and equilibrium was achieved at 0.71 (F_∞). (C) Secondary plot of the association kinetic data in the absence of ATP. k_{obs1} and k_{obs2}, representing the fast and slow phases of the association reaction, are plotted as a function of T286A-αCaMKII concentration. The gradient of the linear regression line fit to the data (◆) was 2.0 (± 0.2) × 10^7 M^{-1} s^{-1}, with the intercept at 7.2 ± 1.9 s^{-1}. A horizontal line drawn at 0.78 ± 0.05 s^{-1} marks the isomerization rate. (D) Secondary plot of the association kinetic data in the presence of ATP. The gradient of the linear regression line fit to the data (◆) was 2.0 (± 0.2) × 10^7 M^{-1} s^{-1}, with the intercept at 9.4 ± 1.2 s^{-1} and to the data (■) 2.3 (±0.1) × 10^6 M^{-1} s^{-1} with the intercept at the origin. The isomerization rate was 0.57 ± 0.05 s^{-1} (---).. The isomerization rate was 0.57 ± 0.05 s^{-1}. (E) Displacement of Ca^{2+}/TA-cal by pig brain Ca^{2+}/calmodulin from its complex with αCaMKII. The equilibrated mixture of 25 nM Ca^{2+}/TA-cal and 250 nM T286A-αCaMKII was rapidly mixed with 2.5 μM Ca^{2+}/calmodulin (mixing chamber concentrations). A biphasic fluorescence change occurred. The exponential rate of the first decreasing phase, k_{diss1}, was 6.0 ± 0.9 s^{-1}, and that of the second rising phase, k_{diss2}, was 0.16 ± 0.01 s^{-1}. (F) Displacement of Ca^{2+}/TA-cal by Ca^{2+}/calmodulin from its complex with αCaMKII in the presence of ATP. The equilibrated mixture of 25 nM Ca^{2+}/TA-cal, 250 nM αCaMKII, and 0.5 mM ATP was rapidly mixed with 2.5 μM Ca^{2+}/calmodulin (mixing chamber concentrations). A monophasic fluorescence change occurred. The exponential rate of the rising phase, k_{diss}, was 0.015 s^{-1}.

intermediates has relative fluorescence <1. The simplest mechanism to explain these data is one in which the formation of an initial complex (described by rate constants k_{+1}, k_{-1}) is followed by isomerization to a second complex (k_{+2}, k_{-2}). According to such a mechanism, where $k_{+2} + k_{-2}$ is 0.78 s^{-1}, taking the observed rates of dissociation and the amplitudes of the fluorescence changes into account as described in ref *24* gives the following parameter values to fit the data: $k_{+1} = 2.0 \times 10^7$ M^{-1} s^{-1}, $k_{-1} = 5.0$ s^{-1}, $k_{+2} = 0.66$ s^{-1}, $k_{-2} = 0.12$ s^{-1}, $F_1 = 1$, $F_2 = 1.50$, and $F_3 = 0.93$.

An alternative scheme consistent with our data represents the formation of two independent Ca^{2+}/TA-cal.T286A complexes, as shown in Scheme 1.

Scheme 1

$$\underset{F_1}{Ca^{2+}/\text{TA-cal.}\alpha\text{T286A}} \underset{k_{-1}}{\overset{k_{+1}}{\rightleftharpoons}} \underset{F_2}{Ca^{2+}/\text{TA-cal}} + \alpha\text{T286A} \underset{k_{-2}}{\overset{k_{+2}}{\rightleftharpoons}} \underset{F_3}{Ca^{2+}/\text{TA-cal.}\alpha\text{T286A}^*}$$

Table 2: Kinetic Parameters of the Interactions of Ca^{2+}/TA-cal and Ca^{2+}/DA-cal with T286A-αCaMKII and Nucleotides in Terms of Schemes 1 and 2

	k'_{+1} (s^{-1})	k'_{-1} (M^{-1} s^{-1})	k'_{+2} (M^{-1} s^{-1})	k'_{-2} (s^{-1})	k_{isom} (s^{-1})	K_{d1} (M)[c]	K_{d2} (M)[d]	K_d (M)[e]	F_1	F'_2	F'_3
Ca^{2+}/TA-cal											
+ αCaMKII[a]	3.52	2.0×10^7	3.2×10^6	0.343	0.78	2.5×10^{-7}	1.1×10^{-7}	7.6×10^{-8}	1	1.40	1.04
+ αCaMKII + ATP[a]	5.0	2.0×10^7	3.2×10^6	0.0027	0.75	2.5×10^{-7}	8.4×10^{-10}	8.4×10^{-10}	1	1.26	0.60
+ T286A	5.0	2.0×10^7	3.2×10^6	0.15	0.79[b]	2.5×10^{-7}	4.7×10^{-8}	3.95×10^{-8}	1	1.50	0.93
+ T286A + ATP	5.0	2.0×10^7	3.2×10^6	0.015	0.70[b]	2.5×10^{-7}	4.7×10^{-9}	4.6×10^{-9}	1	1.38	0.71
Ca^{2+}/DA-cal											
+ αCaMKII	5.83	2.0×10^7	2.5×10^6	1.8 ± 0.2	5.0 ± 0.8	2.5×10^{-7}	7.2×10^{-7}	$9.7 (\pm 0.5) \times 10^{-8}$	1	1	0.53
+ αCaMKII + ATP	5.0	2.0×10^7	$2.50 (\pm 0.12) \times 10^6$	$\leq 6 \times 10^{-5}$	nd[f]	2.5×10^{-7}	$\leq 2.4 \times 10^{-11}$	$\leq 2.4 \times 10^{-11}$	1	1	0.18
+ T286A	5.0	2.0×10^7	$1.8 (\pm 0.1) \times 10^6$	0.05	nd	2.5×10^{-7}	2.8×10^{-8}	2.5×10^{-8}	1	1	0.40
+ T286A + ATP	5.0	2.0×10^7	$2.8 (\pm 0.4) \times 10^6$	0.0022	0.83 ± 0.06	2.5×10^{-7}	7.9×10^{-10}	7.9×10^{-10}	1	1	0.20
+ T286A + AMP-PNP	5.0	2.0×10^7	$6.9 (\pm 0.1) \times 10^5$	0.06	0.6 ± 0.2	2.5×10^{-7}	8.7×10^{-8}	6.5×10^{-8}	1	1	0.30

[a] Best-fit values to Schemes 1 and 2 of data in ref *17*. [b] Values calculated from the formula $k_{isom} = (k'_{+1}k'_{+2} + k'_{-1}k'_{-2})/(k'_{-1} + k'_{+2})$ (*20*). [c] K_{d1} corresponds to k'_{+1}/k'_{-1}. [d] K_{d2} corresponds to k'_{-2}/k'_{+2}. [e] K_d corresponds to $K_{d1}/(1 + K_{d1}/K_{d2})$. [f] nd, not determined.

This mechanism was first analyzed in detail by Bagshaw et al. (*30*) and discussed in ref *24* as one that is often difficult to distinguish from that referred to above, for example, when only one concentration-dependent process is measurable by a fluorescence change. One of the complexes, the more highly fluorescent Ca^{2+}/TA-cal.T286A, would form more rapidly and dissociate more rapidly. The second complex, Ca^{2+}/TA-cal.T286A*, would have fluorescence <1, and would form and dissociate more slowly. Formation of the second complex thus would depend on dissociation of the first complex, the equilibration of the two complexes giving the observed slow isomerization. Dissociation of Ca^{2+}/TA-cal.T286A would represent the first, decreasing phase of fluorescence change, leaving the Ca^{2+}/TA-cal.T286A* complex to dissociate slowly with a rise of fluorescence to 1. This mechanism is shown in Scheme 1. A set of values that fit the data are $k_{+1} = 5.0\ s^{-1}$, $k_{-1} = 2.0 \times 10^7\ M^{-1}\ s^{-1}$, $k_{+2} = 3.2 \times 10^6\ M^{-1}\ s^{-1}$, $k_{-2} = 0.12\ s^{-1}$, $F_1 = 1$, $F_2 = 1.50$, $F_3 = 0.93$. Although the concentration dependence of the formation of the Ca^{2+}/TA-cal.T286A* complex is not seen, the data are consistent with the mechanism shown in Scheme 1; thus, this mechanism cannot be ruled out for the interaction of Ca^{2+}/TA-cal with T286A enzyme.

In the presence of ATP, similar biphasic association kinetics were observed (Figure 2B). Upon closer examination of the second phase of the Ca^{2+}/TA-cal fluorescence change in the association reaction, however, it became evident that the second phase of Ca^{2+}/TA-cal fluorescence change was better fit with two exponentials than with one. Such analysis revealed that the second phase was composed of a concentration-dependent process and a concentration-independent process. As shown in Figure 2D, the gradient of the concentration-dependent process was $2.3 (\pm 0.1) \times 10^6\ M^{-1}\ s^{-1}$. Slow isomerization occurred at $0.45 \pm 0.05\ s^{-1}$. This analysis thus provided evidence for the mechanism shown in Scheme 2.

Scheme 2

$$\underset{F'_2}{Ca^{2+}/\text{TA-cal}.\alpha\text{T286A.ATP}} \rightleftharpoons \underset{F_1}{Ca^{2+}/\text{TA-cal} + \alpha\text{T286A.ATP}} \rightleftharpoons \underset{F'_3}{Ca^{2+}/\text{TA-cal}.\alpha\text{T286A.ATP}^*}$$

(with k'_{+1}, k'_{-1} for the first equilibrium and k'_{+2}, k'_{-2} for the second)

In this model, Ca^{2+}/TA-cal.T286A.ATP forms rapidly, while Ca^{2+}/TA-cal.T286A.ATP* is formed more slowly, and the formation of the Ca^{2+}/TA-cal.T286A.ATP* complex requires dissociation of the Ca^{2+}/TA-cal.T286A.ATP complex. The Ca^{2+}/TA-cal.T286A.ATP* complex is the stable form after equilibration, and the measured dissociation rate constant of $0.015\ s^{-1}$ represents its dissociation. A set of parameters that fit the data are $k'_{+1} = 5.0\ s^{-1}$, $k'_{-1} = 2.0 \times 10^7\ M^{-1}\ s^{-1}$, $k'_{+2} = 3.2 \times 10^6\ M^{-1}\ s^{-1}$, $k'_{-2} = 0.015\ s^{-1}$, $F_1 = 1$, $F'_2 = 1.38$, and $F'_3 = 0.71$. Equilibration of the first and second complexes would appear as an isomerization the rate, which is given as $k_{isom} = (k'_{+1}k'_{+2} + k'_{-1}k'_{-2})/(k'_{-1} + k'_{+2})$ (*24*). This gives an isomerization rate for the T286A αCaMKII mutant in the absence of ATP of $0.79\ s^{-1}$, in excellent agreement with our measured rate of $0.78\ s^{-1}$ (Figure 2C). The isomerization rate calculated for the complex in the presence of ATP is $0.70\ s^{-1}$. This is in reasonable agreement with the measured value of $0.45\ s^{-1}$, considering that the value of k'_{+1} is estimated to be identical to that measured for ATP-free conditions.

K_d values are distinct for the complexes in Schemes 1 and 2: the first complex has $K_{d1} = 2.5 \times 10^{-7}$ M both with and without ATP; the second complex has $K_d = 4.7 \times 10^{-7}$ M in the absence and 4.6×10^{-9} M in the presence of ATP. ATP binding thus stabilized the Ca^{2+}/TA-cal.T286A-αCaMKII complex 9-fold (Table 2).

Steady-State Fluorescence of Ca^{2+}/DA-cal in T286A-αCaMKII Complexes. Changes in global Ca^{2+}/calmodulin conformation can be monitored in real time using DA-cal, a double-mutant (T34C,T110C)-calmodulin labeled with a donor−acceptor pair of probes (*17*, *31*). The donor (AEDANS) equilibrium fluorescence emission intensities of DA-cal (at $\lambda = 490$ nm) free in solution were compared with those of DA-cal in complex with T286A mutant or αCaMKII or $\alpha\text{CaMKII}_{281-319}$ peptide, T286A mutant in the presence of AMP-PNP, and αCaMKII in the presence of ATP. Figure 3 shows the fluorescence emission spectra of DA-cal. In the presence of EGTA (60 nM free Ca^{2+}, record 1), the fluorescence was maximum (relative fluorescence 1.16). In the presence of 0.5 mM Ca^{2+} (record 2), the DA-cal fluorescence was reduced (relative fluorescence 1). Binding to 1.1 μM αCaMKII (record 3) caused a 15% reduction (relative fluorescence 0.85). Binding of DA-cal to 1 μM T286A mutant (record 4) caused a 60% decrease in fluorescence (relative fluorescence 0.40), and binding in the presence of 1.5 mM AMP-PNP (record 5) caused a 68%

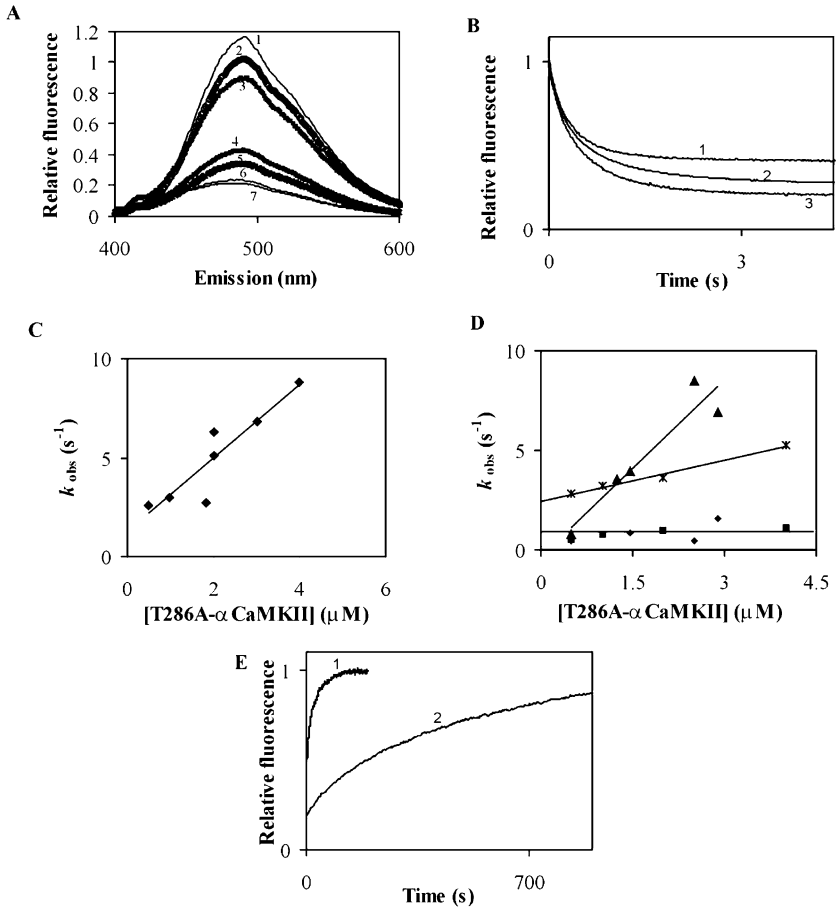

FIGURE 3: Interactions of Ca^{2+}/DA-cal with T286A mutant αCaMKII. (A) Fluorescence emission spectra of the following complexes of 0.2 μM DA-cal and T286A mutant or wild-type αCaMKII at concentrations specified below by steady-state at 21 °C: 1, free DA-cal in the presence of 2 mM EGTA; 2, in the presence of 0.5 mM Ca^{2+}; 3, in complex with 1.1 μM αCaMKII; 4, in complex with 1 μM T286A mutant; 5, with 1 μM T286A mutant and 2 mM AMP-PNP; 6, with 1 μM T286A mutant and 2 mM ATP; and 7, with 1 μM $\alpha CaMKII_{281-319}$ peptide. (B) Association kinetics of the T286A mutant and Ca^{2+}/DA-cal in the presence and in the absence of nucleotides. For record 1, 0.35 μM Ca^{2+}/DA-cal was mixed with 0.60 μM T286A; $k_{obs} = 3.2 \pm 0.1\ s^{-1}$. For record 2, 0.35 μM Ca^{2+}/DA-cal was mixed with 3.8 μM T286A and 1.5 mM AMP-PNP; $k_{obs1} = 2.5 \pm 0.1\ s^{-1}$ (amplitude 0.65) and $k_{obs2} = 0.5 \pm 0.02$ (amplitude 0.35). For record 3, 0.1 μM Ca^{2+}/DA-cal was mixed with 1.25 μM T286A and 0.25 mM ATP; $k_{obs1} = 3.5 \pm 0.2\ s^{-1}$ (amplitude 0.84) and $k_{obs2} = 0.49 \pm 0.08\ s^{-1}$ (amplitude 0.16). (C) Secondary plot of k_{obs} of Ca^{2+}/DA-cal association with T286A-αCaMKII in the absence of nucleotide. The gradient of the linear regression line fit to the data (◆) was 1.8 (± 0.1) × $10^6\ M^{-1}\ s^{-1}$. The intercept was at $1.67\ s^{-1}$. (D) Secondary plot of k_{obs} of Ca^{2+}/DA-cal association with T286A-αCaMKII in the presence of ATP (▲,◆) and AMP-PNP (×,■). The gradients of the linear regression line fit to the data were 2.8 (± 0.4) × $10^6\ M^{-1}\ s^{-1}$ (intercept at 0) when ATP was present and 6.9 (± 0.1) × $10^5\ M^{-1}\ s^{-1}$ (intercept at 2.45 s^{-1}) when AMP-PNP was included. The isomerization rate was $0.83 \pm 0.06\ s^{-1}$ with ATP present (marked by solid line) and $0.6 \pm 0.2\ s^{-1}$ in the presence of AMP-PNP. (E) Dissociation kinetics of Ca^{2+}/DA-cal from its T286A-αCaMKII complex by pig brain calmodulin. For record 1, the equilibrated mixture of 0.5 μM T286A and 0.2 μM Ca^{2+}/DA-cal was mixed with 2.5 μM pig brain Ca^{2+}/calmodulin. The rate of fluorescence increase was $0.050 \pm 0.003\ s^{-1}$. For record 2, the equilibrated mixture of 0.5 μM T286A, 1 mM ATP, and 0.2 μM Ca^{2+}/DA-cal was mixed with 2.5 μM pig brain Ca^{2+}/calmodulin. The rate of fluorescence increase was $0.0022 \pm 0.0001\ s^{-1}$.

reduction in fluorescence (relative fluorescence 0.32). Finally, binding to 1 μM T286A mutant in the presence of 2 mM ATP (record 6) caused a 78% fluorescence reduction (relative fluorescence 0.22), and similarly binding to 1 μM $\alpha CaMKII_{281-319}$ peptide (record 7) caused an 80% fluorescence reduction (relative fluorescence 0.20).

Thus, the data show that, in spectroscopic terms, different complexes of Ca^{2+}/DA-cal with nucleotide-free T286A-αCaMKII compared to nucleotide-bound T286A-αCaMKII are formed. Furthermore, Ca^{2+}/DA-cal fluorescence quenching was greater in the presence of the T286A mutant (relative fluorescence 0.4) than that with the wild-type αCaMKII (relative fluorescence 0.7 (*17*)). Finally, the complex of Ca^{2+}/DA-cal.$\alpha CaMKII_{281-319}$ peptide was spectroscopically similar to that of Ca^{2+}/DA-cal.ATP-bound T286A mutant enzyme.

Ca^{2+}/DA-cal Interactions with T286A-αCaMKII and the Effect of ATP Binding Studied by Stopped-Flow Kinetics. The kinetics of the conformational change of Ca^{2+}/DA-cal during association with and dissociation from nucleotide-free and nucleotide-bound T286A-αCaMKII complexes were investigated in fluorescence stopped-flow experiments in order to understand the mechanism of Ca^{2+}/calmodulin binding to the enzyme. Control experiments showed that none of the nucleotides affected DA-calmodulin fluorescence by themselves (data not shown). Figure 3B shows the Ca^{2+}/DA-calmodulin fluorescence changes in association reactions with T286A-αCaMKII mutant. The rate and amplitude (given in parentheses) as well as the % quenching of DA-cal fluorescence or relative fluorescence for each reaction follow: (i) T286A mutant with no nucleotide added (record 1, $k_{obs} = 3.2 \pm 0.1\ s^{-1}$), amplitude corresponds to 60% of maximal fluorescence quenching or relative fluorescence 0.4; (ii) T286A and 1.5 mM AMP-PNP (record 2, $k_{obs1} = 2.5 \pm 0.1\ s^{-1}$, amplitude 0.65, and $k_{obs2} = 0.5 \pm 0.02\ s^{-1}$, amplitude

0.35), total amplitude corresponds to 70% of maximal fluorescence quenching or relative fluorescence 0.30; and (iii) T286A mutant in the presence of 0.25 mM ATP (record 3, $k_{obs1} = 3.52 \pm 0.24$ s^{-1}, amplitude 0.84, and $k_{obs2} = 0.49 \pm 0.08$ s^{-1}, amplitude 0.16), total amplitude corresponds to 80% of fluorescence quenching or relative fluorescence 0.2.

Thus, the stopped-flow data revealed that Ca^{2+}/DA-cal fluorescence was more quenched in the presence of T286A mutant (Figure 3B) than with αCaMKII (*17*), as was also shown by the steady-state fluorescence data (Figure 3A). ATP caused maximum quenching of Ca^{2+}/DA-cal fluorescence in complex with T286A mutant without Thr_{286}-autophosphorylation (Figure 3B).

In the absence of nucleotides, the DA-cal fluorescence decrease was well fit by a single exponential. The observed rate (k_{obs}) was dependent on enzyme concentration in the range studied with T286A mutant (Figure 3C), with a gradient of 1.5 ($\pm$ 0.1) $\times$ 10^6 M^{-1} s^{-1} for the T286A mutant enzyme (Table 2). Thus, T286A mutant differed from wild-type αCaMKII, for which the observed rate constant (k_{obs}) remained unchanged as a function of αCaMKII concentrations, showing a plateau at 5 s^{-1} (*17*).

The association kinetics of Ca^{2+}/DA-cal with T286A mutant in the presence of ATP showed biphasic fluorescence decay. In Figure 3D, the observed rates of DA-cal conformational change are plotted as a function of T286A mutant concentration. The initial fast phase (k_{obs1}) showed a linear dependence on enzyme concentration in the range studied. The apparent second-order rate constant was 2.8 ($\pm$ 0.4) $\times$ 10^6 M^{-1} s^{-1} for T286A mutant (Table 2). This rate constant was close to that ((2.50 $\pm$ 0.12) $\times$ 10^6 M^{-1} s^{-1}) previously determined for αCaMKII (*17*). The slow phase was independent of enzyme concentration, with $k_{obs2} = 0.83 \pm 0.06$ s^{-1} for T286A mutant enzyme (Figure 3D, Table 2).

DA-cal conformational change was also biphasic during association of Ca^{2+}/DA-cal with T286A-αCaMKII and AMP-PNP, with one phase (k_{obs1}) dependent on enzyme concentration, with gradient 6.9 ($\pm$ 0.1) $\times$ 10^5 M^{-1} s^{-1}, and the other phase concentration independent, with $k_{obs2} = 0.6 \pm 0.2$ s^{-1} (Figure 3D), corresponding to k'_{+2} and k_{isom} in Scheme 2, respectively (Table 2).

Ca^{2+}/DA-cal dissociation rates were measured in displacement reactions with pig brain Ca^{2+}/calmodulin. In the absence of nucleotide, a Ca^{2+}/DA-cal fluorescence increase occurred at 0.05 s^{-1} (Figure 3E, record 1). In the presence of nucleotides, the rates of Ca^{2+}/DA-cal displacement from its complex with T286A mutant were 0.0022 (ATP; Figure 3E, record 2) and 0.06 s^{-1} (AMP-PNP; data not shown). AMP-PNP thus did not have a significant effect on the rate of Ca^{2+}/DA-cal dissociation. The data, however, show that while AMP-PNP slightly destabilizes the complex, ATP binding stabilized the T286A-αCaMKII mutant complex by reducing the rate of Ca^{2+}/DA-cal dissociation 23-fold.

Mechanism of Interactions of Ca^{2+}/DA-cal with T286A-αCaMKII and Its Complexes with ATP and AMP-PNP. In the absence of nucleotide, association of Ca^{2+}/DA-cal with T286A-αCaMKII showed monophasic Ca^{2+}/DA-cal fluorescence quenching with a rate that was essentially independent of the concentration of T286A-αCaMKII; however, as shown in Figures 3B and 4D, Ca^{2+}/DA-cal fluorescence quenching was biphasic in the presence of ATP and AMP-PNP, with k_{obs1} linearly dependent on enzyme concentration and k_{obs2} independent of T286A-αCaMKII mutant concentration. The data can be interpreted in terms of Schemes 1 and 2, in the absence and in the presence of nucleotide, respectively (*24*, *30*). In this case, Ca^{2+}/DA-cal binding to T286A-αCaMKII or to T286A-αCaMKII.ATP appeared to occur without a fluorescence change, whereas the second complex, Ca^{2+}/DA-cal.T286A-αCaMKII* or Ca^{2+}/DA-cal.T286A-αCaMKII.ATP*, had a relative fluorescence of 0.4 or 0.2, respectively. The gradient of k_{obs1} gave a second-order rate constant (k'_{+2}) of 2.8 $\times$ 10^6 M^{-1} s^{-1} in the presence of ATP (Figure 3D). k_{obs2} corresponds to the isomerization at 0.83 s^{-1}, similar to that obtained with TA-cal (Table 2). Data obtained with AMP-PNP could be interpreted in a similar way, with $k'_{+2} = 6.9 \times 10^5$ M^{-1} s^{-1} and isomerization at 0.6 $\pm$ 0.2 s^{-1} (Table 2). Thus, in terms of Schemes 1 and 2, values for the dissociation constants K_d for Ca^{2+}/DA-cal complexes with T286A-αCaMKII mutant, T286A-αCaMKII.ATP, and T286A-αCaMKII.AMP-PNP were calculated as 2.9 $\times$ 10^{-8}, 7.9 $\times$ 10^{-10}, and 6.5 $\times$ 10^{-8} M, respectively (Table 2).

DISCUSSION

Steady-State Characterization of T286A-αCaMKII Enzyme. The T286A mutation has been widely used to study the structure/function relationship of the αCaMKII enzyme in vitro and in vivo (reviewed in refs *1*, *2*; see also refs *6*, *7*, *9*, *11*−*14*, *16*, *17*, *19*, *20*, *32*, *33*). In this study, the T286A mutant of αCaMKII was characterized in the steady state and compared with the wild-type enzyme. The dependence of the specific activities of the T286A mutant and αCaMKII on the concentrations of substrates (MLC and ATP) and activator calmodulin was determined. Both enzymes catalyzed phosphorylation of MLC in the presence of Ca^{2+}/calmodulin and ATP under steady-state conditions (*17*). The maximum activity (V_{max}) of the mutant enzyme was 126 $\pm$ 8 nmol min^{-1} mg^{-1}, whereas that of the wild-type enzyme was 866 $\pm$ 76 nmol min^{-1} mg^{-1} (Table 1). Overall, the (6 $\pm$ 2)-fold difference measured in V_{max} for the two enzymes differs from previous reports that present the two kinases as equally 100% active (*19*). It may be, though, that this difference in activity is a consequence of the substitution of T286A residue with A in the mutant enzyme. Our V_{max} of αCaMKII is higher compared to previously reported values for MLC as substrate (*34*, *35*).

The activities of both enzymes were totally dependent on the presence of Ca^{2+}/calmodulin. Determination of the K_m for calmodulin was difficult due to practical limitations. It was not possible to work at a low enough enzyme concentration to measure K_m. $S_{0.5}$ for activation by Ca^{2+}/calmodulin was estimated to be <100 nM (Table 1). This value for the T286A mutant is in agreement with previously published values of 50−150 nM, depending on the experimental conditions, of the activation constant K_{act} for calmodulin, determined in other studies for wild-type αCaMKII (*32*, *35*−*37*). As can be seen in Figure 1B, Ca^{2+}/calmodulin at concentrations >3 μM appeared to inhibit MLC phosphorylation, suggesting that a second calmodulin molecule may bind with lower affinity.

The activities of both wild-type and mutant αCaMKII showed sigmoid dependence on MLC concentration, indicat-

ing positive cooperativity (Table 1). The K_m values for MLC were determined to be 96 ± 28 μM for T286A mutant and 49 ± 29 μM for αCaMKII. These values are consistent with those reported in the literature for purified rat brain CaMKII (*34*, *35*). The positive cooperativity may be due to an interaction of the substrate-binding domain with the calmodulin-binding domain, as the calmodulin-binding domain is part of a kinase domain that possesses autoinhibitory properties of pseudosubstrate (*38*) or bisubstrate (*33*) nature with regard to its molecular interaction with the catalytic domain of αCaMKII. However, cooperativity may arise as a result of intersubunit substrate phosphorylation, consistent with the two-fold symmetry observed in the αCaMKII dodecamer (*3*, *4*). The 2-fold increase in K_m for MLC caused by the mutation of T286 to A indicates that the A insertion possibly causes a conformational change or a partial displacement of the autoregulatory domain which lowers the affinity for MLC. It thus suggests that the T286 residue may be part of or may affect the conformation of the protein substrate-binding domain. It also indicates that substrate specificity may be affected by conformational changes in the region of the T286 residue.

The rates of MLC phosphorylation by αCaMKII and T286A mutant as a function of the concentration of ATP showed a hyperbolic dependence. The best-fit values for V_{max} at 100 μM MLC were 99 ± 7 nmol min^{-1} mg^{-1} for T286A mutant and 440 ± 37 nmol min^{-1} mg^{-1} for αCaMKII (Table 1). Our $S_{0.5}$ values (Table 1) are consistent with others previously published for wild-type αCaMKII using different substrates (*33*, *34*, *39*, *40*). K_m for ATP was 2.4-fold lower in the T286A mutant than in the wild-type αCaMKII enzyme. This may be the effect of the changes this mutation causes to the calmodulin binding site and affinity. As shown by our kinetic analysis, K_d for calmodulin was approximately 2-fold lower in T286A-αCaMKII. Our data further show that ATP increased the affinity for calmodulin. It is thus expected that calmodulin binding increases the affinity for ATP. There appears to be an interdomain interaction between the two sites (*17*). The decrease in K_m for calmodulin by the T286A mutant enzyme thus may reflect the decreased K_d for calmodulin.

The 7-fold lower activity of the T286A mutant enzyme compared to that of the wild-type αCaMKII was accompanied by a 2-fold difference in the K_m for ATP. Overall this indicates that, since the autoregulatory domain overlaps with the calmodulin-binding domain and the latter overlaps with the substrate-binding domain, the A insertion in the regulatory domain affects calmodulin binding, which in turn may change the specificities of the substrate- and ATP-binding domains.

Effect of ATP Binding to Ca^{2+}/Calmodulin Conformation and Binding to T286A-αCaMKII without Thr$_{286}$-Autophosphorylation. ATP caused stabilization of Ca^{2+}/calmodulin binding to T286A mutant by reducing the rate of Ca^{2+}/calmodulin dissociation from the ATP-bound T286A-αCaMKII complex, as was shown in experiments using both fluorescent calmodulins (TA-cal and DA-cal) (Table 2). The presence of ATP reduced the dissociation constant K_d of T286A mutant enzyme to Ca^{2+}/calmodulin by 9- and 21-fold, as revealed by experiments using TA-cal and DA-cal, respectively. Ca^{2+}/TA-cal association experiments with the T286A mutant enzyme showed similar association rate constants (k_{+1}) in the absence and in the presence of ATP. The isomerized Ca^{2+}/calmodulin.αT286A.ATP* complexes were strongly favored in the presence of ATP, as was shown by Ca^{2+}/TA-cal dissociation kinetic experiments as well as by Ca^{2+}/DA-cal steady-state fluorescence experiments. This finding also is applicable to the wild-type αCaMKII (*17*).

Furthermore, our data show that ATP binding itself to T286A-αCaMKII without Thr$_{286}$-autophosphorylation induces changes in the global conformation of Ca^{2+}/calmodulin. Distinct complexes of Ca^{2+}/DA-cal upon interaction with T286A-αCaMKII are reported. The structure of Ca^{2+}/DA-cal is more compacted with the T286A mutant than with the wild-type enzyme, as reported in ref *17*. AMP-PNP and ATP binding caused intermediate and maximum compaction of T286A-bound Ca^{2+}/DA-cal conformation, respectively. In these complexes, the Ca^{2+}/calmodulin conformation is more compact and/or the equilibrium between the initial and compacted complexes is shifted toward the compacted form. The Ca^{2+}/DA-cal conformation also appears maximally compact when bound to the αCaMKII$_{281-319}$ peptide and Thr$_{286}$-phospho-αCaMKII. These results reveal multiple Ca^{2+}/calmodulin conformations, which may have a direct effect on the regulation of the T286A-αCaMKII activity, similar to that of the wild-type αCaMKII (*17*).

The stabilization of Ca^{2+}/calmodulin binding to the T286A αCaMKII mutant by ATP is likely to be applicable to the wild-type enzyme as well, although the ATP-bound intermediate undergoes Thr$_{286}$-autophosphorylation and is thus not readily isolated. Moreover, a reciprocal stabilization of ATP binding by Ca^{2+}/calmodulin is expected. Calmodulin binding has previously been shown to cause a 9-fold increase in the affinity of Mg^{2+}ADP to brain CaMKII (*41*).

Interactions of T286A-αCaMKII with Ca^{2+}/Calmodulin and ATP and Implications for the Activation Mechanism of αCaMKII. As discussed above, T286A mutant binding to Ca^{2+}/DA-cal caused 60% quenching of its fluorescence as opposed to 30% quenching caused by αCaMKII binding. The mechanism of interaction of Ca^{2+}/DA-cal with the T286A mutant was analogous to that with αCaMKII, with two main differences. First, the equilibrium between the two complexes, defined by the isomerization, was strongly biased to the second complex, in which Ca^{2+}/DA-cal was bound in a more compact conformation than in the case of αCaMKII (*17*). Second, the Ca^{2+}/DA-cal dissociation constant for the T286A mutant was 3-fold reduced compared to that for the αCaMKII enzyme, revealing previously undetected subtle differences between the wild-type and mutant enzymes, making the T286A mutant enzyme more similar to phospho-Thr$_{286}$-αCaMKII than previously thought (*19*). A left shift in the Ca^{2+} dependence of the activity and Ca^{2+} dissociation kinetics similar to those of phospho-Thr$_{286}$-αCaMKII are consistent with higher affinity for Ca^{2+}/calmodulin by the T286A mutant compared to the wild-type enzyme (A. Tzortzopoulos and K. Török, unpublished data). While the equilibrium between the Ca^{2+}/DA-cal.αCaMKII and Ca^{2+}/DA-cal.αCaMKII* complexes is well poised, in the case of the T286A mutant it is biased toward the second complex of lower fluorescence. The dissociation constant (K'_{d2}) of the Ca^{2+}/DA-cal.αT286A* complex is 22-fold lower than that for the wild-type enzyme (Table 2).

Taken together, the observations made with TA-cal and DA-cal suggest the following model, consistent with the data obtained with both probes in the presence of nucleotide ATP or AMP-PNP: two independent complexes, Ca^{2+}/cal.αT286A.ATP and Ca^{2+}/cal.αT286A.ATP*, are formed. The TA-calmodulin fluorescence increase is characteristic of the formation of the Ca^{2+}/cal.αT286A.ATP complex (Scheme 2, $k'_{-1} = 2.0 \times 10^7$ M^{-1} s^{-1}). In this complex, calmodulin remains in an extended conformation, not detected by DA-cal. The Ca^{2+}/cal.αT286A.ATP* complex is formed with rate constant $k'_{+2} = 3 \times 10^6$ M^{-1} s^{-1}. This is seen as calmodulin compaction by DA-cal (Figure 3C,D) and as the first phase of TA-cal fluorescence decrease which follows the initial increase (Figure 2D). The slow isomerization measured by both probes corresponds to equilibration of the Ca^{2+}/cal.αT286A.ATP and Ca^{2+}/cal.αT286A.ATP* complexes (Table 2).

The lower rate of 6.9×10^5 M^{-1} s^{-1} with AMP-PNP is probably related to the different nature of the non-physiological and non-hydrolyzable nucleotide. In studies characterizing the interaction of non-physiological nucleotides with enzymes, a lower affinity of AMP-PNP binding to nucleoside diphosphate (NDP) kinases was measured (*42*).

The models presented are applicable to the activation of αCaMKII by calmodulin and ATP (*17*, *43*). One of the complexes formed by Ca^{2+}/cal, αCaMKII, and ATP would represent an unproductive complex with incorrectly bound calmodulin. This may occur if, for example, calmodulin is associated with the binding region of the enzyme in opposite polarity compared to the productive complexes, in which calmodulin binding is stabilized in a collapsed conformation.

The Ca^{2+}/cal.αT286A intermediates involved in the activation mechanism can be related to those suggested for wild-type αCaMKII (*17*). In the absence of nucleotide, the formation of two Ca^{2+}/cal.αT286A complexes (species 2a and 2b in ref *17*) is shown to occur by the mechanism of rapid Ca^{2+}/calmodulin binding followed by isomerization; however, it is not possible to exclude the mechanism shown in Scheme 2, in which the two complexes form independently. In the presence of ATP, the mechanism demonstrated for the T286A mutant enzyme corresponds to that shown in Scheme 2 and can be related to that suggested for the wild-type enzyme (*17*), where the two complexes of Ca^{2+}/cal, αT286A, and ATP correspond to species 3a and 4a (*17*). The rate constants consistent with the mechanism in Scheme 2 for αCaMKII and T286A mutant αCaMKII are listed in Table 2. It is likely that only one of the two complexes is on the activation pathway, and thus the formation of an unproductive complex may play a key role as rate-controlling steps in subsequent activation of αCaMKII. Our kinetic data are consistent with the existence of a T286A-αCaMKII.ATP complex; however, it remains to be determined whether a random or ordered mechanism governs the activation process.

In conclusion, different kinetic properties of the T286A mutant compared with those of the wild-type αCaMKII were revealed. ATP binding to T286A mutant without the interference of Thr_{286}-autophosphorylation increases the affinity of the enzyme for Ca^{2+}/calmodulin and induces significant changes to the structure of T286A-αCaMKII-bound Ca^{2+}/calmodulin complex.

REFERENCES

1. Lisman, J., Schulman, H., and Cline, H. (2002) The molecular basis of CaMKII function in synaptic behavioural memory, *Nat. Rev. Neurosci. 3*, 175−190.
2. Soderling, T. R., Chang, B., and Brickey, D. (2001) Cellular signalling through multifunctional Ca^{2+}/calmodulin-dependent protein kinase II, *J. Biol. Chem. 276*, 3719−3722.
3. Morris, E. P., and Török, K. (2001) Oligomeric structure of α-calmodulin-dependent protein kinase II, *J. Mol. Biol. 308*, 1−8.
4. Kolodzej, S. J., Hudmon, A., Waxham, M. N., and Stoops, J. K. (2000) Three-dimensional reconstructions of Ca^{2+}/calmodulin-dependent (CaM) protein kinase IIα and truncated CaM kinase IIα reveal a unique organisation for its structural core and functional domains, *J. Biol. Chem. 275*, 14354−14359.
5. Bliss T. V. P., and Collinridge G. L. (1993) A synaptic model of memory: long-term potentiation in the hippocampus, *Nature 361*, 31−39.
6. Shen, K., and Meyer, T. (1999) Dynamic control of CaMKII translocation and localization in hippocampal neurons by NMDA receptor stimulation, *Science 284*, 162−166.
7. Colbran R. J. (2003) Targeting of calcium/calmodulin-dependent protein kinase II, *Biochem J. 378*, 1−16.
8. Ehlers, M. D., Zhang, S., Bernhadt, J. P., and Huganir, R. L. (1996) Inactivation of NMDA receptors by direct interaction of calmodulin with the NR1 subunit, *Cell 84*, 745−55.
9. Barria, A., Muller, D., Derkach, V., Griffith, L. C., and Soderling, T. R. (1997) Regulatory phosphorylation of AMPA-type glutamate receptors by CaM-KII during long-term potentiation, *Science 267*, 2042−2045.
10. Hayashi, Y., Shi, S. H., Esteban, J. A., Piccini, A., Poncer, J. C., and Malinow, R. (2000) Driving AMPA receptors into synapses by LTP and CaMKII: requirement for GluR1 and PDZ domain interaction, *Science 287*, 2262−2267.
11. Silva, A. J., Paylor, R., Wehner, J. M., and Tonegawa, S. (1992) Deficient hippocampal long-term potentiation in alpha-calcium-calmodulin kinase II mutant mice, *Science 257*, 206−210.
12. Frankland, P. W., O'Brien, C., Ohno, M., Kirkwood, A., and Silva, A. J. (2001) Alpha-CaMKII-dependent plasticity in the cortex is required for permanent memory, *Nature 411*, 309−313.
13. Giese, K. P., Fedorov, N. B., Filiplowski, R. K., and Silva, A. J. (1998) Autophosphorylation at Thr286 of the alpha calcium-calmodulin kinase II in LTP and learning, *Science 279*, 870−873.
14. Hardingham, N., Glazewski, S., Pakhotin, P., Mizuno, K., Chapman, P. F., Giese, K. P., and Fox, K. (2003) Neocortical long-term potentiation and experience-dependent synaptic plasticity require alpha-calcium/calmodulin-dependent protein kinase II autophosphorylation, *J. Neurosci. 23*, 4428−4436.
15. Shields, S. M., Vernon, P. J., and Kelly, P. T. (1984) Autophosphorylation of calmodulin-kinase II in synaptic junctions modulates endogenous kinase activity, *J. Neurochem. 43*, 1599−1609.
16. Meyer, T., Hanson, P. I., Stryer, L., and Schulman, H. (1992) Calmodulin trapping by calcium/calmodulin-dependent protein kinase, *Science 256*, 1199−1202.
17. Török, K., Tzortzopoulos, A., Grabarek, Z., Best, S., and Thorogate, R. (2001) Dual effect of ATP in the activation mechanism of brain Ca^{2+}/calmodulin-dependent protein kinase II by Ca^{2+}/calmodulin, *Biochemistry 40*, 14878−14890.
18. Miller, S. G., and Kennedy, M. B. (1986) Regulation of brain type II Ca^{2+}/calmodulin-dependent protein kinase by autophosphorylation: a Ca^{2+}-triggered molecular switch, *Cell 44*, 861−870.
19. Fong, Y.-L., Taylor, W. L., Means, A. R., and Soderling, T. R. (1989) Studies of the regulatory mechanism of Ca^{2+}/calmodulin-dependent protein kinase II. Mutation of threonine 286 to alanine and aspartate, *J. Biol. Chem. 264*, 16759−16763.
20. Bayer, K.-U., De Koninck, P., Leonard, S., Hell, J. W., and Schulman, H. (2001) Interaction with the NMDA receptor locks CaMKII in an active conformation, *Nature 411*, 801−805.
21. Katoh, T., and Fujisawa, H. (1991) Calmodulin-dependent protein kinase II. Kinetic studies on the interaction with substrates and calmodulin, *Biochim. Biophys. Acta 1091*, 205−212.
22. Kwiatkovski, A. P., Huang, C. Y., and King, M. M. (1990) Kinetic mechanism of the type II calmodulin-dependent protein kinase: studies of the forward and reverse reactions and observation of apparent rapid-equilibrium ordered binding, *Biochemistry 29*, 153−159.

23. Lengyel, I., Nairn, A. C., McCluskey, A., Toth, G., Benke, B., and Rostas, J. A. P. (2001) Auto-inhibition of Ca^{2+}/calmodulin-dependent protein kinase II by its ATP-binding domain, *J. Neurochem. 76*, 1066−1072.
24. Török K., and Trentham, D. R. (1994) Mechanism of 2-Chloro-(ϵ-amino-Lys_{75})-[6-[4-(*N*,*N*-diethylamino)phenyl]-1,3,5-triazin-4-yl]calmodulin interactions with smooth muscle myosin light chain kinase and derived peptides, *Biochemistry 33*, 12807−12820.
25. Rowe, T., and Kendrick-Jones, J. (1992) Chimeric myosin regulatory light chains identify the subdomain responsible for regulatory function, *EMBO J. 11*, 4715−4722.
26. Gill, S. C., and von Hippel, P. H. (1989) Calculation of protein extinction coefficients from amino acid sequence data, *Anal. Biochem. 182*, 319−326.
27. Bradford, M. M. (1976) A rapid and sensitive method for the quantitation of microgram quantities of protein utilizing the principle of protein−dye binding, *Anal. Biochem. 72*, 248−254.
28. Török, K., Cowley, D. J., Brandmeier, B. D., Howell, S., Aitken, A., and Trentham, D. R. (1998) Inhibition of calmodulin-activated smooth-muscle myosin light chain kinase by calmodulin-binding peptides and fluorescent (phosphodiesterase-activating) calmodulin derivatives, *Biochemistry 37*, 6188−6198.
29. Török, K., Thorogate, R., and Howell, S. (YEAR) in *Calcium-Binding Protein Protocols*, *Vol. 2: Methods and Techniques* (Vogel, H. J., Ed.) Methods in Molecular Biology 173, pp 383−407, Humana Press Inc., Totowa, NY.
30. Bagshaw, C. R., Eccleston, J. F., Eckstein, F., Goody, R. S., Gutfreund, H., and Trentham, D. R. (1974) The magnesium ion-dependent adenosine triphosphatase of myosin: two-step processes of adenosine triphosphate association and dissociation, *Biochem. J. 141*, 351−364.
31. Drum, C. L., Yan, S.-Z., Sarac, R., Mabuchi, Y., Beckingham, K., Bohm, A., Grabarek, Z., and Tang, W.-J. (2000) An extended conformation of calmodulin induces interactions between the structural domains of adenylyl cyclase from *Bacillus anthracis* to promote catalysis, *J. Biol. Chem. 275*, 36334−36340.
32. Mukherji, S., and Soderling, T. R. (1995) Mutational analysis of Ca^{2+}-independent autophosphorylation of calcium/calmodulin-dependent protein kinase II, *J. Biol. Chem. 270*, 14062−14067.
33. Brickey, D. A., Bann, J. G., Fong, Y.-L., Perrino, L., Brennan, R. G., and Soderling, T. R. (1994) Mutational analysis of the autoinhibitory domain of calmodulin kinase II, *J. Biol. Chem. 269*, 29047−29054.
34. Yamamoto, H., Fukunaga, K., Goto, S., Tanaka, E., and Miyamoto, E. J. (1985) Ca^{2+}, calmodulin-dependent regulation of microtubule formation via phosphorylation of microtubule-associated protein 2, tau factor, and tubulin, and comparison with the cyclic AMP-dependent phosphorylation, *J. Neurochem. 44*, 759−768.
35. Kuret, J., and Schulman, H. (1984) Purification and characterization of a Ca^{2+}/calmodulin-dependent protein kinase from rat brain, *Biochemistry 23*, 5495−5504.
36. Brickey, D. A., Colbran, R. J., Fong, Y.-L., and Soderling, T. R. (1990) Expression and characterization of the alpha-subunit of Ca^{2+}/calmodulin-dependent protein kinase II using the baculovirus expression system, *Biochem. Biophys. Res. Commun. 173*, 578−584.
37. Waxham, M. N., Aronowski, J., and Kelly, P. T. (1989) Functional analysis of Ca^{2+}/calmodulin-dependent protein kinase II expressed in bacteria, *J. Biol. Chem. 264*, 7477−7482.
38. Cruzalegui, F. H., Kapiloff, M. S., Morfin, J.-P., Kemp, B. E., Rosenfeld, M. G., and Means, A. R. (1992) Regulation of intrasteric inhibition of the multifunctional calcium/calmodulin-dependent protein kinase, *Proc. Natl. Acad. Sci. U.S.A. 89*, 12127−12131.
39. Colbran, R. J. (1993) Inactivation of Ca^{2+}/calmodulin-dependent protein kinase II by basal autophosphorylation, *J. Biol. Chem. 268*, 7163−7170.
40. Ahmad, Z., DePaoli-Roach, A. A., and Roach, P. J. (1982) Purification and characterization of a rabbit liver calmodulin-dependent protein kinase able to phosphorylate glycogen synthase, *J. Biol. Chem. 257*, 8348−8355.
41. King, M. M., Shell, D. J., and Kwiatkowski, A. P. (1988) Affinity labeling of the ATP-binding site of type II calmodulin-dependent protein kinase by 5′-p-fluorosulfonylbenzoyl adenosine, *Arch. Biochem. Biophys. 267*, 467−473.
42. Cervoni, L., Lascu, I., Xu, Y., Gonin, P., Morr, M., Merouani, M., Janin, J., and Giartosio, A. (2001) Binding of nucleotides to nucleoside diphosphate kinase: a calorimetric study, *Biochemistry 40*, 4583−4589.
43. Török, K. (2002) Calmodulin conformational changes in the activation of protein kinases, *Biochem. Soc. Trans. 30*, 55−61.

BI036224M